Quaternary Geochronology 91 (2026) 101712

Contents lists available at ScienceDirect

Quaternary Geochronology

journal homepage: www.elsevier.com/locate/quageo

Chronological horizon of Weichselian submoraine organic formation and macrofossil finds with radiocarbon and tree-ring $\delta^{18}O$ analyses

Markku Oinonen [a,*], Laura Arppe [a], Joonas Uusitalo [a], Samuli Helama [b], Pekka Nöjd [c], Harri Mäkinen [c], Pekka Saranpää [d], Kenichiro Mizohata [e]

[a] Finnish Museum of Natural History, P.O.Box 64, 00014, University of Helsinki, Finland
[b] Natural Resources Institute Finland, Ounasjoentie 6, 96200, Rovaniemi, Finland
[c] Natural Resources Institute Finland, Latokartanonkaari 9, 00790, Helsinki, Finland
[d] Natural Resources Institute Finland, Viikinkaari 9, 00790, Helsinki, Finland
[e] Department of Physics, P.O.Box 64, 00014, University of Helsinki, Finland

ARTICLE INFO

Keywords:
Northern Finland
Weichselian
Peat formation
Radiocarbon
Oxygen isotopes
Chronology
Marine isotope stages

ABSTRACT

Detailed chronological assessment has been performed on a strongly compressed submorainic organic layer found from a river valley in the Lemmenjoki area, Northern Finland, by using ^{14}C and $\delta^{18}O$ analyses. Clear effect of reworked carbon from above has been observed within the basal part of the layer. The radiocarbon data combined with existing chronological information suggest that the layer was deposited during the Marine Isotope Stage 3 (MIS3), supporting the previously published interpretation. Particularly, most of the dates are indistinguishable from the ^{14}C background level, indicating their association with the early phase of MIS3 time period. Oxygen isotopic data resembles the data from the last 400 years within the eastern Fennoscandia, suggesting similar growth conditions during the period compared to modern era.

1. Introduction

Organic matter deposits store information on their age and interglacial/interstadial climate and environmental conditions and thus provide multidimensional views to the past, supplementing the knowledge of Quaternary climate variability largely based on marine sediment and ice core records. Oxygen isotopic ratios of ice cores, particularly, provide well-established framework for paleoenvironmental studies of the last glacial era (Fig. 1). Based on this chronological and isotopic setting, studies of the glacial history of the northern Europe/European Arctic has been studied through analyses of interglacial and interstadial deposits focusing on the MIS3 (Martinson et al., 1987). An increasing number of sediment successions has been analyzed to detail the climatic and vegetation development demonstrating ice-free interstadial conditions for the northern Europe (Alexanderson et al., 2009; Hättestrand and Robertsson, 2010; Helmens, 2014; Lunkka et al., 2008, 2015, 2008; Mäkinen, 2005; Salonen et al., 2008, 2014; Sarala et al., 2010, 2016; Sarala and Eskola, 2011; Väliranta et al., 2009).

Although the Greenland ice core $\delta^{18}O$ records (Andersen et al., 2004; Rasmussen et al., 2023) show (Fig. 1) clearly cooler conditions during the Weichselian interstadials compared to Holocene and Eemian interglacial climates, plant macrofossil (Väliranta et al., 2009), modeling (Van Meerbeeck et al., 2011) and palynological (Helmens, 2014) analyses indicate significantly warmer interstadial conditions in northern Europe. Recently, indications of even forested environment were observed at the site of Kaarreoja in Northern Finland associated to Marine Isotope Stage 3 (MIS3) interstadial (Sarala et al., 2016) of ca. 24–59 cal kBP (Martinson et al., 1987). The Kaarreoja site (Fig. 2) has been subject to extensive gold mining excavations that have produced a set of isolated finds of wood suggested to originate from an organic layer underlying Holocene fluvial sand deposit (MIS1) and sandy till and glaciofluvial sand layers (MIS2). Such an organic layer is a major storage of chronological, environmental and climatic information since organic material has fixed both carbon and oxygen isotopes through its photosynthetic production. For example, stable oxygen isotope ratios ($\delta^{18}O$) of tree-ring cellulose allow for assessments of prevailed climatic conditions by storing the isotopic signature of source water containing temperature information (McCarroll and Loader, 2004; Roden et al., 2000).

* Corresponding author. Finnish Museum of Natural History, P.O.Box 64, 00014, University of Helsinki, Finland.
E-mail addresses: markku.j.oinonen@helsinki.fi (M. Oinonen), laura.arppe@helsinki.fi (L. Arppe), joonas.uusitalo@helsinki.fi (J. Uusitalo), samuli.helama@luke.fi (S. Helama), pekka.nojd@luke.fi (P. Nöjd), harri.makinen@luke.fi (H. Mäkinen), pekka.saranpaa@luke.fi (P. Saranpää), kenichiro.mizohata@helsinki.fi (K. Mizohata).

https://doi.org/10.1016/j.quageo.2025.101712
Received 23 September 2024; Received in revised form 3 November 2025; Accepted 5 November 2025
Available online 10 November 2025

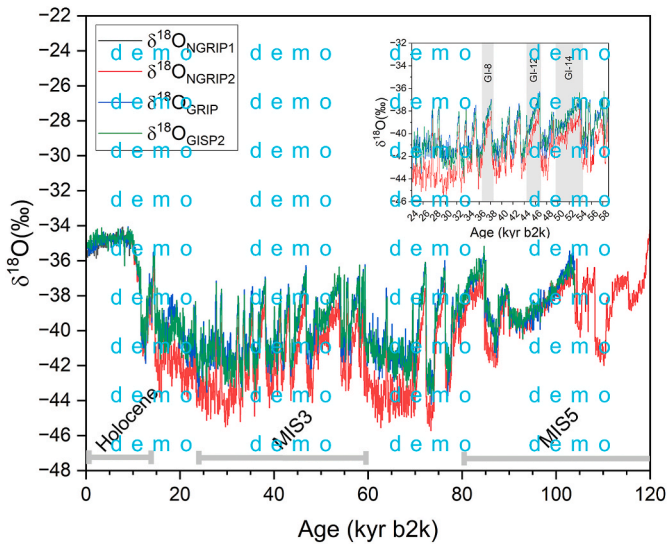

Fig. 1. Chronological and oxygen isotopic setting of the last glacial era of Greenland. The data is based on https://www.iceandclimate.nbi.ku.dk/data/(Rasmussen et al., 2014, 2023). The insert shows approximately the period of Marine Isotope Stage 3 (MIS3). Note that age unit of "year b2k" links to "year cal BP" via relation year b2k = year cal BP + 50.

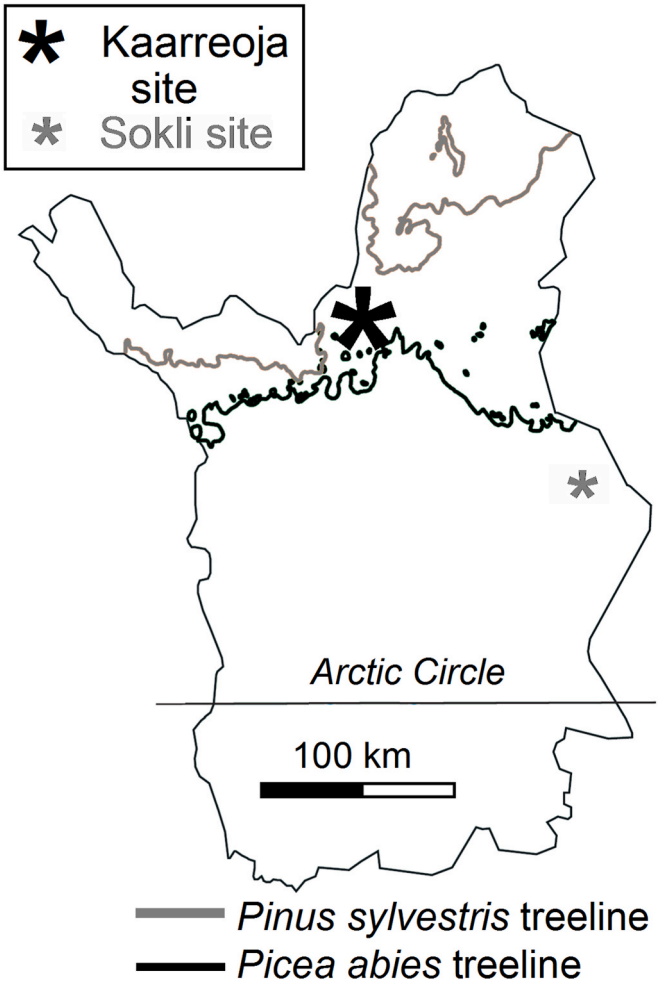

Fig. 2. Study site of Kaarreoja within Northern Finland shown by black symbol. Sokli site mentioned in the text has also been shown by smaller grey symbol.

With regards of the assumed MIS3 deposits, extraction of geochronometric information may come with challenges due to nearly negligible amount of radiocarbon (^{14}C) at the temporal vicinity of the methodological detection limit.

In this work, we address the organic layer found from the Kaarreoja site by merging ^{14}C and δ^{18}O data of the identified wood macrofossils, and by dating of twig macrofossils and bulk gyttja/peat across the layer to understand the site chronology close to the detection limit of the ^{14}C methodology. First, we aim to understand the methodological issues inevitably faced in close-to-background radiocarbon analyses. Second, we aim to resolve whether the organic layer was formed during a mid-Weichselian MIS3 interstadial or earlier interglacial/interstadial phases. If the layer is from MIS3, it would potentially provide an interesting opportunity to advance towards broader studies of environmental phases and events dated to MIS3, such as the latest reversal of the Earth's magnetic field i.e. the Laschamp event (Bonhommet and Zähringer, 1969) ca. 42000 years ago, and to produce northern ^{14}C calibration data close to the methodological sensitivity limit. We hope that this work emphasizes the role of northern Finland and the Kaarreoja site, in particular, as an invaluable archive of environmental records of the last glacial cycle.

2. Materials and methods

This study has been made through a consortium between University of Helsinki (UH) and Natural Resources Institute Finland (Luke) established in 2010. The consortium contributes to the stable isotopic and radiocarbon measurements using the supra-long tree-ring chronology of northern Finland. The collaborative research involves researchers and facilities from Luke, Finnish Museum of Natural History (Luomus)/UH and Faculty of Sciences/UH. The Luke group is responsible for curating and sampling of the wood material and the Laboratory of Chronology of Luomus has the overall responsibility of the ^{14}C analytical process including chemical pretreatment, combustion and graphitization of samples. The ^{14}C content determinations on the graphite samples are performed at the Helsinki Accelerator Mass Spectrometry (HAMS) facility of the Department of Physics, Faculty of Sciences/UH. The full description of the ^{14}C measurement process for wood cellulose within the University of Helsinki has been recently published (Uusitalo et al., 2022) including thorough analyses on process backgrounds.

2.1. Samples

Samples (Table 1) were retrieved from still at that time actively excavated sections in the river valley of Kaarreoja, a tributary of the Miessijoki/Miessejohka river system, in northeast Finnish Lapland (68.65°N, 25.65°E, WGS84, see Fig. 2). Our set of samples represents wood specimens of macrofossil to megafossil size, macrofossil twig specimens and peat/gyttja extracted from the submorainic organic deposit. This peat/gyttja layer has been associated previously with the MIS3 interstadial (Sarala et al., 2016). In that work, the stratigraphy of the site (Fig. 3) was published: the studied layer was underlying the Holocenic organic layer (ca. 0.5 m) and fluvial sand deposit (MIS1) and till/glaciofluvial sand layers (MIS2) of ca. 1.5 m. The uppermost part of the organic layer was formed of extremely compressed peat including wood pieces (unit 5 in Sarala et al., 2016, Fig. 3).

Our megafossil-size wood samples (K1-K7) typically of 10–50 cm in length and containing 38–58 annual rings, originate presumably from this organic layer. These samples have been found during gold-mining excavations from different locations of the area and thus should be considered only as representing an overview of the chronological scheme of the site. Thin sections were produced for wood anatomical characterization (Bernabei and Bontadi, 2011; Hellberg and Carcaillet, 2016; Kozakiewicz and Zyczkowski, 2015; Schweingruber, 1990).

Our studied section of mostly gyttja represents the unit 4, which Sarala et al. (2016) described as comprising organic gyttja and wood

Table 1
Sample data for the Kaarreoja site.

Layer (pos.)	Material	Sample	Species	Lab code	Pret.	Comb. & Graph.	AMS	Ref.
mineral below organic	quartz			Hel-TL04274	N/A	N/A	N/A	Sarala et al. (2016)
organic	wood			Hela-2693	AAA	CTC	Uppsala	Sarala et al. (2016)
organic	bulk peat			Tln-3277	N/A	N/A	N/A	Sarala et al. (2016)
organic	wood	K1	*Picea abies*	Hela-3994	AAA	CTC	Helsinki	this work
organic	wood	K2	*Picea abies*	Hela-4244	cellulose	EA-HASE	Helsinki	this work
organic	wood	K3	*Picea abies*	Hela-4245	cellulose	EA-HASE	Helsinki	this work
organic	wood	K4	*Picea abies*	Hela-4246	cellulose	EA-HASE	Helsinki	this work
organic	wood	K5	*Juniperus communis*	Hela-4247	cellulose	EA-HASE	Helsinki	this work
organic	wood	K6	*Juniperus communis*	Hela-4248	cellulose	EA-HASE	Helsinki	this work
organic	wood	K7	*Betula* sp.	Hela-4508	cellulose	EA-HASE	Helsinki	this work
organic (13–15 cm)	gyttja/peat	G1		Hela-4440	AAA, insoluble/humin	EA-HASE	Helsinki	this work
organic (13–15 cm)	gyttja/peat	G1		Hela-4440/3	AAA, insoluble/humin	EA-HASE	Helsinki	this work
organic (24–26 cm)	gyttja/peat	G2		Hela-4441	AAA, insoluble/humin	EA-HASE	Helsinki	this work
organic (31–33 cm)	gyttja/peat	G3		Hela-4442	AAA, insoluble/humin	EA-HASE	Helsinki	this work
organic (41–43 cm)	gyttja/peat	G4		Hela-4443	AAA, insoluble/humin	EA-HASE	Helsinki	this work
organic (57–59 cm)	gyttja/peat	G5		Hela-4444	AAA, insoluble/humin	EA-HASE	Helsinki	this work
organic (13–15 cm)	twig/wood	T1	indet.	Hela-4477	AAA	EA-HASE	Helsinki	this work
organic (24–26 cm)	twig/wood	T2	indet.	Hela-4478	AAA	EA-HASE	Helsinki	this work
organic (31–33 cm)	twig/wood	T3	indet.	Hela-4479	AAA	EA-HASE	Helsinki	this work
organic (41–43 cm)	twig/wood	T4	indet.	Hela-4480	AAA	EA-HASE	Helsinki	this work
organic (57–59 cm)	twig/wood	T5	indet.	Hela-4481	AAA	EA-HASE	Helsinki	this work
organic (13–15 cm)	gyttja/peat	H1		Hela-4440/2	AA, soluble/humic	EA-HASE	Helsinki	this work
organic (24–26 cm)	gyttja/peat	H2		Hela-4441/2	AA, soluble/humic	EA-HASE	Helsinki	this work
organic (31–33 cm)	gyttja/peat	H3		Hela-4442/2	AA, soluble/humic	EA-HASE	Helsinki	this work
organic (41–43 cm)	gyttja/peat	H4		Hela-4443/2	AA, soluble/humic	EA-HASE	Helsinki	this work
organic (57–59 cm)	gyttja/peat	H5		Hela-4444/2	AA, soluble/humic	EA-HASE	Helsinki	this work

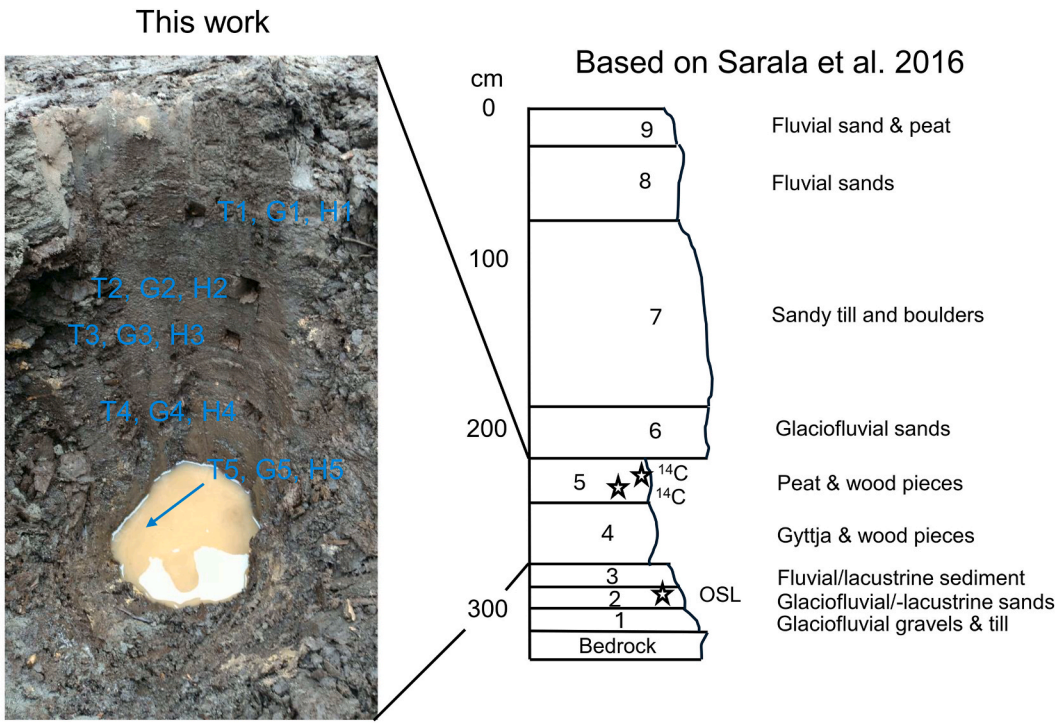

Fig. 3. Left: Sampling locations from the organic layer with sample names indicated. Note the location of T5, G5, H5 samples: after sampling it was immediately covered by water. The samples were taken from locations from which wooden twigs (T) were found. Right: Schematic view on the site stratigraphy based on (Sarala et al., 2016). The star symbols indicate the sampling locations of the existing ^{14}C and OSL dates prior to this work.

pieces and, indeed, contained also macrofossil-sized twigs/shrubs. Five 2x2x2 cm^3 samples of both gyttja (resulting in sample fractions G1-G5, H1-H5) and adjacent macrofossil twigs/shrubs (T1-T5) were collected across this 70 cm thick unit from top to basal layer, at which a transition was observed from gyttja to mineral deposits of probably glaciofluvial or -lacustrine origin representing possibly the units 3 and 2 of Sarala et al. (2016). The sampling locations were defined by observation of twig macrofossils, since this allowed for pairwise comparison of the ^{14}C dating results of terrestrial macrofossils and bulk gyttja. Our hypothetical stratigraphy of units 5 and 4 would mean that the samples from the unit 5 (K1-K7) should be slightly younger than the samples from the unit 4 (G1-G5, T1-T5).

2.2. ^{14}C analyses

To verify the quality of the ^{14}C measurement process wood samples

from the Sixth International Radiocarbon Intercomparison (SIRI) campaign (Scott et al., 2017) were measured and compared to consensus values (Table 2). From the study site altogether 22 ^{14}C measurements were performed (Tables 3 and 4). In addition, there are three existing dating results by ^{14}C and OSL methods from Kaarreoja related to the same layer stratigraphy (Sarala et al., 2016).

High-quality wood samples were chemically pretreated to cellulose (Helama et al., 2015; Uusitalo et al., 2018, 2022) and partially decayed samples with the acid-alkali-acid (AAA) method (de Vries and Barendsen, 1954) to obtain alkali-insoluble (humin) fraction of peat/gyttja samples. In addition, alkali-soluble (humic) fractions from peat/gyttja samples were extracted and dated. Details of the AAA processes are provided in Table 2. After each steps 1–3 of Table 2, solutions were washed to neutrality with MilliQ® water and eventually dried at ca. 90–100 °C. The dried samples were crushed and homogenized for combustion and graphitization processes.

Two AMS graphite target preparation processes, discussed in detail elsewhere (Kasso et al., 2021; Uusitalo et al., 2022), were utilized (Fig. 4). The first uses a labor-intensive closed-tube-combustion (CTC) methodology coupled to Fe/Zn graphitization process for carbon dioxide (Slota et al., 1987). The second is optimized for small (<1 mg carbon target masses) samples and uses elemental analyzer (EA; Thermo Scientific Flash, 2000 NC, Thermo Fisher Scientific Inc., Waltham, MA, USA) for fast combustion and similarly a catalytic (Zn/Fe) reduction process for graphitization with Labview-controlled HASE reactors (Palonen et al., 2013). The latter and the mostly used process is referred as EA-HASE (Fig. 4). The obtained graphite + Fe samples were pressed into AMS cathodes (2JD032750 Cathode Blank, National Electrostatics Corp., Middleton, WI, USA) by using a pneumatic sample press (PSP, Ionplus AG, Dietikon, Switzerland). Oxalic acid II samples (NIST SRM 4990C) were used as a standard material. Eventually, the ^{14}C concentrations were measured with the Helsinki AMS (HAMS) facility (Palonen and Tikkanen, 2015; Tikkanen et al., 2004) on the graphite targets by utilizing a Bayesian data-analysis approach (Palonen et al., 2010a), provided as fraction modern values (Donahue et al., 1990) and converted to radiocarbon ages. The Bayesian process allows for integral assessment of the HAMS machine characteristics thus resulting in more realistic uncertainties compared to the typical mean-based method (Palonen, 2008a).

Each batch of 40 samples at UH includes a pressed ^{14}C-dead natural graphite (14734 Graphite powder, −200 mesh, 99.9999 %, Alfa Aesar, Karlsruhe, Germany) target and a large-mass blank (lmb) (Donahue et al., 1990) target of either combusted and graphitized natural graphite (as above) or combusted and graphitized fossil diesel sample for CTC (N = 13 since 3/2017) and EA-HASE (N = 24, since 3/2017), respectively. The latter samples allow for controlling the both batch-specific and mean background for the combustion – graphitization – AMS process (Uusitalo et al., 2022). Background-corrected fraction modern values are obtained through an equation $F = F_{uncorr}\bullet(1+ f_{lmb}) - f_{lmb}$ (Palonen, 2008b), in which f_{lmb} = lmb background correction, F_{uncorr} = uncorrected fraction modern of a sample and F = fraction modern of a sample corrected for lmb background. Typically, to reduce a role of potential outliers, the background is deduced as weighed average of multiple lmb-background measurements so that the weights of the earlier backgrounds decrease exponentially by factor of 0.68. In this work, however, we used the mean value of all the lmb background measurements as an average background for the study period of 2017–2020.

Potential mass-dependent background corrections were estimated according to our recent study (Uusitalo et al., 2022). Particularly, sample mass-dependent effects may cause slight systematic correction into ^{14}C concentrations due to assumed constant amount of modern carbon involved within sample preparation phases that bring in more ^{14}C particularly for old samples (Uusitalo et al., 2022). We note that our estimation of this so-called mass-balance-blank (mbb) correction is based on only several samples (Uusitalo et al., 2022) and thus our correction is tentative and is used as sensitivity analysis only. Furthermore, during the measurement campaigns in 2017–2020, the full process (cellulose extraction – combustion – graphitization – AMS) background was monitored with a cellulose sample from ^{14}C-dead wood (*Larix*, 30/KAM/79) assumed to be from Eem interglacial (Mäkinen, 1982).

One-tailed two-sample z test was used for statistical comparisons. Particularly, the measured F_{uncorr} was compared to mean ($f_{lmb,\ mean}$) background values to obtain a measure for statistical significance of its difference from the ^{14}C background. If statistical significance was obtained ($p < 0.05$, null hypothesis: $f_{lmb} = F_{uncorr}$), the background-corrected value (F) was converted to radiocarbon age as $-8033\bullet\ln(F)$. Asymmetric uncertainty estimates for the radiocarbon age were obtained as $-8033\bullet\ln(F \pm \sigma)$ in which σ = half-width of the 68.3 % central posterior density interval, corresponding to the standard deviation of the assumed Gaussian distribution of the mean-based ^{14}C data-analysis method (Palonen et al., 2010b; Uusitalo et al., 2022). Alternatively, if significance was not obtained ($p > 0.05$), a lower limit for an age was estimated following the conventions adopted by the ^{14}C community as $> -8033\bullet\ln(F_{limit}) = -8033\bullet\ln(F + 2\sigma)$ and by setting F = 0 in case it is negative (van der Plicht and Hogg, 2006). Throughout the work, radiocarbon ages are referred to with the unit of BP and calendar ages with the unit of cal BP i.e. calendar years back in time counted from the year 1950. This converts to ice core chronologies with age unit of "year b2k" with a formula of year b2k = year cal BP + 50. Conversion of radiocarbon ages to calendar years is performed by using the IntCal20 calibration curve (Reimer et al., 2020). This curve reaches 55000 cal BP calendar year limit and this means that the oldest radiocarbon age to be converted to calendar years is 50100 BP (Reimer et al., 2020).

Table 2
Details of acid-alkali-acid (AAA) pretreatment processes for the studied samples. Details of the subsequent cellulose sample treatment have been described by Uusitalo et al. (2022).

Material	Samples	Lab codes	1st phase	2nd phase	3rd phase
wood		Hela-2693	>3h 0.57M HCl @ 90–100 °C	4h 0.5M NaOH @ 90–100 °C	1–2h 0.29M HCl @ 90–100 °C
wood	K1	Hela-3994	>3h 0.57M HCl @ 90–100 °C	4h 0.5M NaOH @ 90–100 °C	1–2h 0.29M HCl @ 90–100 °C
gyttja/peat	G1-G5	Hela-4440-4444	>3h 0.57M HCl @ 90–100 °C	3–4h 0.25M NaOH @ 90–100 °C	1–2h 0.29M HCl @ 90–100 °C
gyttja/peat	G1	Hela-4440/3	6h 0.57M HCl @ 90–100 °C	2 × 4h 0.5M NaOH @ 90–100 °C	2h 0.29M HCl @ 90–100 °C
gyttja/peat	H1-H5	Hela-4440/2–4444/2	6h 0.57M HCl @ 90–100 °C	3–4h 0.5M NaOH @ 90–100 °C	
twigs	T1-T5	Hela-4477-4481	7h 0.57M HCl @ 90–100 °C	2 × 4h 0.5M NaOH @ 90–100 °C	2h 0.29M HCl @ 90–100 °C

2.3. Stable isotopic analyses

For isotopic analysis of oxygen of the alpha-cellulose, a sample of ca. 300 μg was weighed into a high-purity silver capsule (IVA Analysentechnik 99.99 % Ag capsule). The capsules were crimped to remove all air and loaded alongside reference cellulose materials into a Costech zero-blank autosampler, subsequently sealed and flushed with He to protect the samples and the analysis from the effects of atmosphere. Analysis was conducted on a Thermo Scientific EA-Isolink system, consisting of a Flash IRMS elemental analyser/pyrolysis unit and a Delta V Plus isotope ratio mass spectrometer linked via the ConFlo IV system. All samples were analyzed in triplicate, and the mean oxygen isotope value is reported. The sample replicates showed standard deviation systematically below ±0.14 ‰. The isotope values are reported conventionally as δ^{18}O values, as permil differences from the V-SMOW

Table 3
Results of the measurements of reference samples from the Sixth International Radiocarbon Intercomparison (SIRI) (Scott et al., 2017). "2" in the Lab code refers to additional acid (A) wash during 2021 on previously (for SIRI) extracted cellulose samples. The results are given as background-corrected F values and the consensus values (F_{cons}) as the estimates based on mixed effects model (Scott et al., 2017). Results of the statistical z tests between F and F_{cons} are also given (z, p).

Material	Sample	Lab code	Pret.	Comb. & Graph.	F	σ	F_{cons}	σ_{cons}	z	p
wood	SIRI A	Hela-3348/2	cellulose & A	EA-HASE	0.0002	0.0010	0.0013	0.0017	−0.492	0.311
wood	SIRI E	Hela-3349/2	cellulose & A	EA-HASE	0.2569	0.0011	0.2598	0.0025	−1.106	0.134
wood	SIRI F	Hela-3350/2	cellulose & A	EA-HASE	0.9565	0.0030	0.9550	0.0042	0.303	0.381
wood	SIRI G	Hela-3351/2	cellulose & A	EA-HASE	0.9472	0.0047	0.9540	0.0046	−1.047	0.148
wood	SIRI H	Hela-3352/2	cellulose & A	EA-HASE	0.9513	0.0046	0.9532	0.0042	−0.308	0.379
wood	SIRI I	Hela-3353/2	cellulose & A	EA-HASE	0.2838	0.0014	0.2884	0.0018	−2.087	0.018
wood	SIRI L	Hela-3354/2	cellulose & A	EA-HASE	0.0002	0.0010	0.0011	0.0020	−0.402	0.344

Table 4
Chronological data for the organic layer found from the Kaarreoja site. Oxygen isotopic ratios of the wood cellulose samples K2-K6 are also provided.

Lab code	Sample	f_{lmb}	F_{uncorr}	z score	p(F_{uncorr} vs f_{lmb})	F	RA (BP) or OSL age (a)	$\delta^{18}O$(‰)
Hel-TL04274		N/A	N/A	N/A	N/A	N/A	52000(12000)	
Hela-2693		0.0042(13)	0.0034(11)	−0.448	0.327	−0.0008(18)	> 45200	
Tln-3277		N/A	N/A	N/A	N/A	N/A	30200(250)	
Hela-3994	K1	0.0040(15)	0.0075(4)	2.210	0.014	0.0035(16)	45400^{+4900}_{-3000}	
Hela-4244	K2	0.0026(10)	0.0037(1)	1.118	0.132	0.0012(10)	> 46900	27.4
Hela-4245	K3	0.0026(10)	0.0027(1)	0.169	0.433	0.0002(10)	> 49400	26.7
Hela-4246	K4	0.0026(10)	0.0041(1)	1.498	0.067	0.0016(10)	> 45300	26.8
Hela-4247	K5	0.0026(10)	0.0035(1)	1.023	0.153	0.0010(10)	> 46800	26.9
Hela-4248	K6	0.0026(10)	0.0036(1)	1.023	0.153	0.0011(10)	> 46600	26.5
Hela-4508	K7	0.0026(10)	0.0173(3)	13.547	<0.001	0.0148(11)	33850^{+580}_{-550}	
Hela-4440	G1	0.0026(10)	0.0064(2)	3.632	<0.001	0.0039(11)	44600^{+2500}_{-1900}	
Hela-4440/3	G1	0.0026(10)	0.0036(1)	1.056	0.145	0.0011(10)	> 46500	
Hela-4441	G2	0.0026(10)	0.0059(2)	3.164	0.001	0.0034(11)	45800^{+2900}_{-2200}	
Hela-4442	G3	0.0026(10)	0.0051(2)	2.414	0.008	0.0026(11)	47900^{+4100}_{-2700}	
Hela-4443	G4	0.0026(10)	0.0037(2)	1.103	0.135	0.0012(11)	> 46200	
Hela-4444	G5	0.0026(10)	0.0061(2)	3.351	<0.001	0.0036(11)	45300^{+2700}_{-2100}	
Hela-4477	T1	0.0026(10)	0.0015(1)	−0.970	0.166	−0.0011(10)	> 50000	
Hela-4478	T2	0.0026(10)	0.0012(1)	−1.255	0.105	−0.0014(10)	> 50000	
Hela-4479	T3	0.0026(10)	0.0040(1)	1.384	0.083	0.0015(11)	> 45500	
Hela-4480	T4	0.0026(10)	0.0015(1)	−0.970	0.166	−0.0011(10)	> 50000	
Hela-4481	T5	0.0026(10)	0.0014(1)	−1.065	0.143	−0.0012(10)	> 50000	
Hela-4440/2	H1	0.0026(10)	0.0038(1)	1.258	0.104	0.0013(10)	> 46000	
Hela-4441/2	H2	0.0026(10)	0.0023(1)	−0.257	0.399	−0.0002(10)	> 49900	
Hela-4442/2	H3	0.0026(10)	0.0030(1)	0.450	0.326	0.0005(10)	> 48300	
Hela-4443/2	H4	0.0026(10)	0.0034(1)	0.854	0.196	0.0009(10)	> 47100	
Hela-4444/2	H5	0.0026(10)	0.0168(2)	14.175	<0.001	0.0143(10)	34100^{+700}_{-600}	

standard. Data normalization was based on multiple analyses of a cellulose standard "Hki1" assigned a value of 27.7 ‰. Hki1 is an α-cellulose extracted at the Laboratory of Chronology from a milled and sieved (<80 μg) pine tree powder distributed as wood standard "PF" to nine participating laboratories in an intercomparison study of the ISONET project (Boettger et al., 2007). As a measure of accuracy, replicates of the international secondary IAEA-CH3 yielded a $\delta^{18}O$ value of 32.1(2)‰ (n = 7) during the analytical period.

3. Results

The wood samples of the Sixth International Radiocarbon Intercomparison (SIRI) cover wide time span of from ca. 350 BP to ca. 50 000 BP thus providing a suitable sample set to test the ^{14}C process quality. Out of 7 SIRI sample measurements (Table 3), 6 are not statistically separable from the consensus values and one (I) slightly older (z = −2.087, p = 0.018). Thus, statistically, the ^{14}C measurement process of UH reproduces the SIRI consensus values. Particularly, for SIRI A and L wood samples that have close-to-background ^{14}C concentrations, the EA-HASE-AMS process at UH resulted very low background-corrected F values corresponding to radiocarbon ages of >49200 BP, deduced from F+2σ.

As we use the long-term ^{14}C background in Fig. 5 for comparison, we here summarize the results obtained previously at UH (Uusitalo et al., 2022). Based on a ^{14}C-dead wood sample (*Larix*, 30/KAM/79) the long-term process background for the complete ^{14}C measuring process including cellulose extraction, combustion, graphitization and AMS measurement for EA-HASE process was obtained as $f_{tot} = 0.0036(5)$. The average lmb background (Fig. 5) during the Kaarreoja measurement campaign including combustion, graphitization and AMS measurement, without cellulose extraction, was obtained through fossil diesel measurements as $f_{lmb,\ EA\text{-}HASE} = 0.0026(10)$. Thus, one obtains a cellulose extraction background by subtraction of these two to be $f_{cell} = 0.0010(11)$ (Uusitalo et al., 2022). This actually can also be considered as the lmb-corrected ^{14}C concentration for the 30/KAM/79 sample i.e. $f_{cell} = F_{30/KAM/79}$ to estimate its ^{14}C age: it corresponds to >55100 BP age and, deduced from F + 2σ, to >46400 BP.

According to our wood anatomical analyses four megafossil specimens (K1-K4) represent spruce. In these samples, piceoid pits were identified in the cross-field. Fusiform rays were found with thick-walled resin canal epithelial cells. The sample K4 was characterised by uneven ring structure and could be rootwood. Two specimens (K5-K6) represent juniper with tracheids showing helical cavities in the cell wall in radial sections. In these samples, no fusiform rays were observed. The height of uniseriate rays was very low. Cupressoid pits were found in the cross-field. One sample (K7) represents birch, with uniseriate, biseriate and triseriate rays in radial section. The size of this stemwood specimen shows it represents tree birch. Thus, the megafossil-size specimens represent the variation of the tree species found at the Kaarreoja site.

The results of the chronological data as fraction modern values and

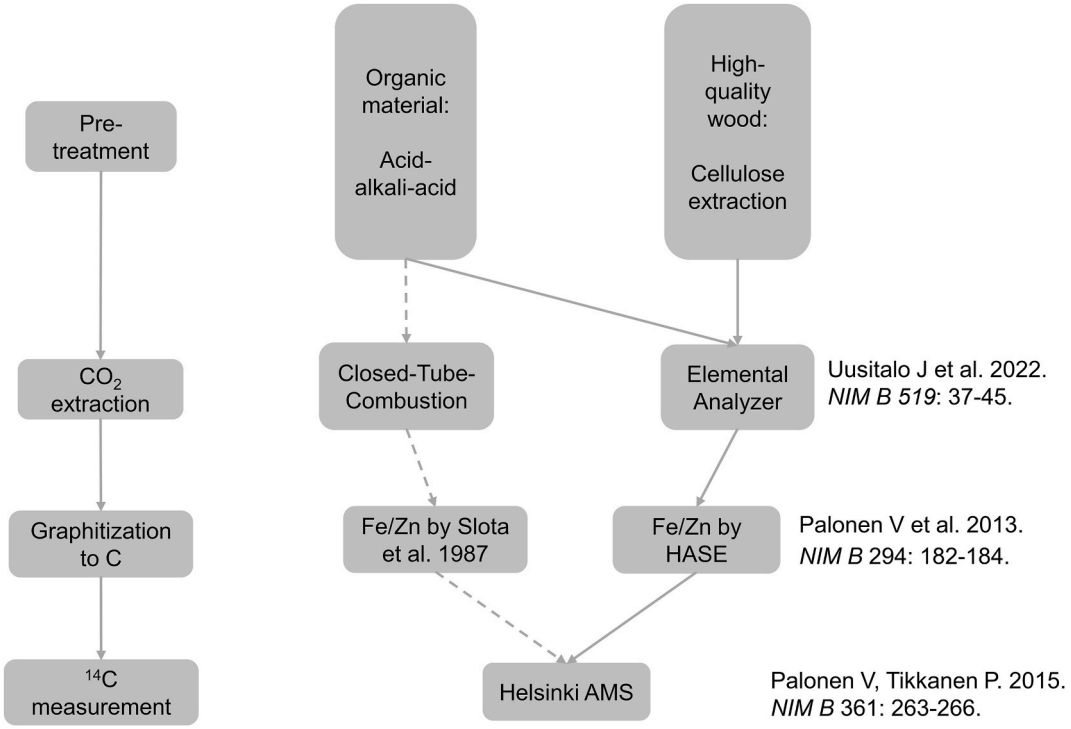

Fig. 4. Schematic illustration of the ^{14}C dating process discussed in the text. Left: Process flow including chemical pretreatment, CO_2 extraction, graphitization and ^{14}C measurement. Right: Actual processes and corresponding literature references, if available. Dashed lines illustrate process flows rarely used.

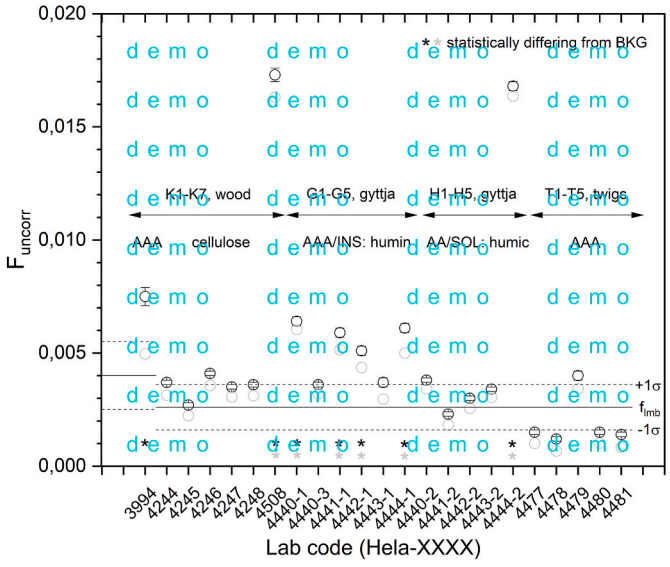

Fig. 5. Comparison of the measured ^{14}C data (F_{uncorr} i.e. uncorrected for ^{14}C background) with the ^{14}C background level (large-mass blank ie. lmb background f_{lmb}). Note that the data for K1 has been obtained with CTC process thus having slightly higher f_{lmb}. x-axis: laboratory codes (Hela-XXXX). Black symbols: F_{uncorr}. Grey symbols: values corrected for sample mass effects (see text). AAA/INS: humin refers to the sample fractions (G1-G5) obtained through the full acid-alkali-acid pretreatment i.e. alkali insoluble fraction. AA/SOL: humic refers to the sample fractions (H1-H5) soluble within the alkali pretreatment step.

in radiocarbon years are summarized in Table 4 and visualized in Fig. 5. The ^{14}C concentrations of the most of the megafossil wood (spruce, juniper, birch) samples from Kaarreoja site (K2-K6) are statistically not distinguishable from the long-term mean background $f_{lmb,\ EA\text{-}HASE}$. Actually, they result in the same mean value than our ^{14}C-free wood sample 30/KAM/79 given above i.e. $F_{uncorr,K2\text{-}K6} = 0.0035(6)$ vs. $f_{tot} = 0.0036(5)$ leading to infinite ages. However, two wood samples (K1, K7) seem to provide finite ages since the ^{14}C concentrations are above the sensitivity limit of the method. Slight differences between ^{14}C contents of the G1-G5, H1-H5 and T1-T5 sample fractions are also observed (Table 4, Fig. 5). Particularly, the bulk gyttja/peat samples (G1-G5), treated with the full acid-alkali-acid (AAA) process, have significantly ($p < 10^{-4}$ for all respective samples) higher ^{14}C concentrations compared to their macrofossil (twig) counterparts (T1-T5) from exactly the same depth. However, when G1 sample was treated with significantly (time x2, strength x2) stronger NaOH pretreatment step (Hela-4440-3) the result was indistinguishable from the background.

Macrofossil twig samples indicate very low ^{14}C contents even below lmb background resulting in infinite ages. Although it seems that these T1-T5 samples - assumedly from the unit 4 (see Fig. 3) - have slightly lower ^{14}C content compared to K2-K6 tree samples (unit 5), the difference between the averages does not reach statistical significance ($z = 1.254$, $p = 0.105$). Sample-mass-dependent corrections (Fig. 5, light grey symbols) reduce the observed ^{14}C contents slightly throughout the data set typically by less than 0.001 fraction modern units, but occasionally more. It is also noteworthy that the gyttja sample fractions closest to the bottom of the layer (G5, H5) have clearly the highest ^{14}C contents among their series thus resulting in younger ages.

Oxygen isotopic ratios ($\delta^{18}O$, Table 4) of K2-K6 wood cellulose (*Picea abies* and *Juniperus communis*) samples range from 26.5 to 27.4 ‰ ($\delta^{18}O_{Kaarreoja,\ mean} = 26.9(4)$ ‰) and do not differ from the value measured for the old 30/KAM/79 wood cellulose (*Larix*) sample of 26.4 ‰. In fact, the range do not differ from the wood cellulose (*Pinus sylvestris*) $\delta^{18}O$ records of the late Holocenic period of AD 1600–2000 from northern (68° 56′ N, 28° 19′ E: $\delta^{18}O_{Kessi,\ mean} = 26.6(7)$ ‰) and eastern Finland (62° 59′ N, 31° 16’ E: $\delta^{18}O_{Sivakkovaara,\ mean} = 27.3(8)$ ‰) either, measured through ISONET collaboration (Hilasvuori et al., 2009).

4. Discussion

4.1. Quality of ^{14}C measurements

Quality of the radiocarbon measurements of wood cellulose within University of Helsinki has been thoroughly discussed elsewhere (Uusitalo et al., 2022). Here we discuss the observed long-term background against new measurements of Sixth International Radiocarbon Intercomparison (SIRI) wood samples. The background-corrected value of the ^{14}C-dead wood sample (*Larix*, 30/KAM/79) $F_{30/KAM/79} = 0.0010$ (11) is similar to the consensus values of the old wood samples (A and L) of SIRI of $F_A = 0.00133(162)$ and $F_L = 0.0011(20)$, respectively (Scott et al., 2017). In addition, our new direct measurements of these SIRI A and L wood samples provide even lower F values (Table 3). Further, altogether 6 out of 7 values measured for SIRI samples chronologically spanning from Middle Ages to the sensitivity limit do not statistically differ from the consensus values (Table 3). Based on above observations we conclude that our radiocarbon measurement process (EA-HA-SE-AMS) for wood cellulose provides equally high quality compared to the overall global average of ^{14}C-AMS laboratories.

The 30/KAM/79 sample has been previously dated to >49200 BP (Su-826) and it has been considered to originate from Eemian interglacial (Mäkinen, 1982). Our results of >55100 BP or (based on F + 2σ) >46400 BP are consistent with the previous estimate. Our close-to-background data raises a question whether MIS3 association would still be possible for the 30/KAM/79 sample.

4.2. Sample mass effects

The megafossil wood samples are isolated finds and thus carry less importance with respect to local stratigraphy. Most of them have ^{14}C content indistinguishable ($p > 0.05$) from ^{14}C background indicating that they may represent either very early MIS3 or earlier interstadial/interglacial conditions. Two measurements of the macrofossils, K1 (Hela-3994) and K7 (Hela-4508), deserve special attention. Both are significantly above the lmb background (Table 4, Fig. 5). However, reduced sample masses of Accelerator Mass Spectrometry (AMS) targets can have pronounced effects particularly on close-to-background measurements (Uusitalo et al., 2022). The mass-dependent effects of these samples are visualized in Fig. 5 (grey symbols) – systematic correction reduces their ^{14}C contents. Particularly, corrections are larger for the CTC process, used for K1 (Hela-3994), compared to EA-HASE, since the EA-HASE process has been volumetrically optimized for smaller samples. Thus, this mass-balance-blank (mbb) correction (Uusitalo et al., 2022) considered, K1 is no longer statistically separable from background. This seems to strengthen the view that the isolated finds from the Kaarreoja site may be relatively old. Eventually, having applied the mbb correction, the only macrofossil wood/twig sample remaining statistically separated from the ^{14}C background is K7. Thus, the examination of the ^{14}C results suggests the presence of *Betula* (K7) in the area ca. 34 kBP (ca. 39 cal kBP) ago, whereas the studied *Picea* and *Juniperus* samples are older.

Alkali-soluble humic (H1-H5) and alkali-insoluble humin (G1-G5) peat/gyttja samples provide slightly younger ages (higher ^{14}C concentrations) compared to the same-depth macrofossil twigs (T1-T5). The samples were quite small with the AMS target masses ranging from 0.25 to 1.1 mg of carbon (mgC). Therefore, it is worth to discuss the effect of mbb correction. In fact, it can be estimated that the mass-dependent effects may explain 10–70 % of the differences observed between the samples as the strength of this effect is increased in the vicinity of the ^{14}C detection limit (Uusitalo et al., 2022). Particularly, as can be seen in Fig. 5, the mbb corrections are largest for the G1-G5 samples which are the smallest in mass (0.25–0.76 mgC). However, still ca. 30–90 % of the difference between the gyttja and twig samples need to be explained by factors other than the sample mass.

4.3. ^{14}C inversion of basal samples

The ^{14}C content of the gyttja (G1-G5) sequence follows a decreasing trend towards the bottom of the organic bed, except that the basal sample (G5) provides again a higher ^{14}C content of $F_{Hela\text{-}4444} = 0.0036$ (11). A similar but even stronger inversion is evident also for the humus sequence (H1-H5): the H5 sample has the highest ^{14}C content of $F_{Hela\text{-}4444/2} = 0.0143(10)$. These ^{14}C trends can be explained by draining of younger gyttja/humus into the bottom from the overlying organic deposits. It has been suspected that drained humic acids or extruded roots could cause younger ages for interstadial/interglacial organic layers (Wohlfarth, 2010) possibly evidenced, for instance, as surprisingly young ^{14}C dates within Eemian or Holsteinian peat layers in Estonia (Kalm, 2006). Further, recent work on close-to-background organic deposits (Palstra et al., 2021) suggests that the percolation of younger humified material from overlying sediments may impact dates more than commonly assumed. Indeed, our test with stronger alkali (NaOH) treatment reduced the ^{14}C content of the alkali-insoluble sample of G1 to the background level. This is in accord with the observations by Palstra et al. (2021), namely that the alkali pretreatment step at higher than room temperature and stronger than 0.2M alkaline solution is required to remove the added carbon fractions. Actually, our test indicates that high temperature (here 90–100 °C) and even stronger solution (here 0.5M, Table 2) may be required to remove the bias of younger carbon. Namely, the stronger treatment reduces the ^{14}C concentration of our test sample (G1) from $F_{Hela\text{-}4440} = 0.0039(11)$ to $F_{Hela\text{-}4440/3} = 0.0011(10)$ (Table 4). So, the stronger alkali pretreatment brings even the gyttja of the highest measured position (G1) to the background level.

In our setting, the basal part represents an organic content in which reworked carbon from overlying organic material seems to significantly contribute to ^{14}C age estimation, with effects that are not totally removed by the pretreatment protocols, except with a sufficiently strong chemical pretreatment. In fact, such a tendency towards younger basal samples is not observed for the twig macrofossil samples T1-T5, probably since stronger 0.5M solution was applied to these samples already. Overall, our work provides quantitative evidence to pay attention to the strength of the chemical pretreatment processes needed to remove the biases from reworked younger carbon in similar settings.

4.4. Chronological assessment of the layer

Since gyttja (G1-G5) and humus (H1-H5) samples suffer from reworked younger carbon we base our chronological assessment to wood macrofossil (K1-K7) samples found from the same layer with different locations and to twig (T1-T5) samples found from one location. The samples result in mostly infinite date limits (Table 4) between >45300 and > 50000 BP, except for K1 (45400^{+4900}_{-3000} BP) and K7 (33850^{+580}_{-550} BP). Particularly, the limits of 45300–50000 BP correspond to calendar ages of ca. 47600–53500 cal BP.

Calendar year conversion allows for comparison to available chronological information on the organic bed and the underlying mineral layer (Fig. 6). Most of the infinite dates older than ca. 47600–53500 cal BP are consistent with the previously published date of wood piece of the peat layer i.e. >47400 cal BP of Hela-2693 (Sarala et al., 2016). That is, similar to most of our isolated finds, the ^{14}C content of wood piece of Sarala et al. (2016) could not be distinguished from the ^{14}C background. Younger finite date of ca. 38700 cal BP (K7, Hela-4508), possibly also other (K1, Hela-3994), indicate that the sedimentation has continued for millenia, this also being consistent with the previous observation (Sarala et al., 2016) of a bulk sample from the middle part of the peat deposit of ca. 35000 cal BP (Tln-3277).

The underlying mineral layer 3 provides a *terminus a quo* for the organic layer chronology (Fig. 3). Unfortunately, only one OSL date (Hel-TL04274) exists for this layer (Sarala et al., 2016) with relatively large uncertainties (52000 ± 12000 a) and thus quantitative estimates,

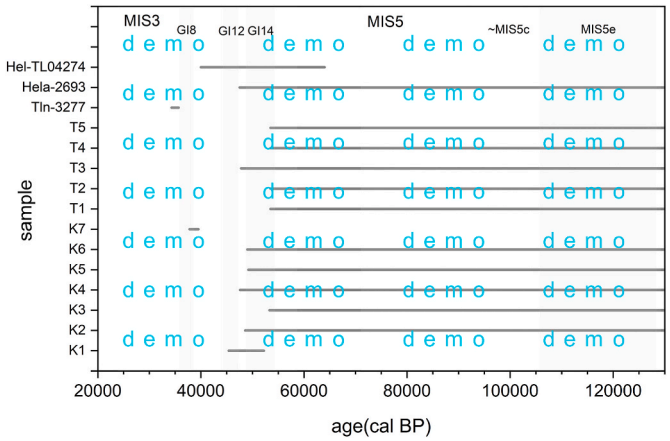

Fig. 6. Summary of the present chronological information on the organic layer of Kaarreoja site expressed as calendar years (calBP) for wood/twig samples. Grey vertical bars illustrate calendar year ranges (1σ for finite ages), grey horizontal lines represent the mean or lower limit value of the extrapolated calendar year probability distributions. The light grey shaded regions represent the estimated periods of MIS3 and MIS5 (Martinson et al., 1987) and dark grey shaded regions the interstadials (Van Meerbeeck et al., 2011) or internal structure of Marine Isotope Stages (Stirling et al., 1998). An estimate for MIS5c has also been given (Väliranta et al., 2009).

to chronologically model the early phases of the boundary of the mineral and organic layers, are still challenging. Nevertheless, such the OSL date is an independent verification of the chronological horizon of the basal gyttja.

The organic layer found from Kaarreoja site has been recently associated with the Marine Isotope Stage (MIS) 3 period (Sarala et al., 2016). However, most of the Kaarreoja macrofossils representing wood or twig samples result in close-to-background ^{14}C content corresponding to infinite ages. Thus, one can also consider a possibility of them resulting from the earlier ice-free periods of the MIS5 period (Fig. 1) such as Eemian interglacial (MIS5e) or early Weichselian Brørup interstadial at ca. 100 cal kBP corresponding to MIS5c (Väliranta et al., 2009). Pollen assemblages of both from northern Finland (Sokli, 67°48′ N, 29°18′E) indicate vegetation similar to the Holocene interglacial (Helmens, 2014) thus further justifying such a consideration.

The origin of the above-discussed reworked carbon is crucial for understanding the chronological horizon of the studied organic layer. As discussed by Palstra et al. (2021), a thick and compressed peat layer may act as a buffer to limit the influence of the percolating carbon from the overlying sediment layers to deeper layers. So, if the studied layer – that was indeed significantly compressed to the extent that all the macrofossil samples were flattened – would be due to MIS3 and prevent the Holocenic humic substances from percolating into it, one should see basal date inversion due to compression of MIS3 organic deposit and thus humic dates of only MIS3 chronological horizon, not younger. On the other hand, if the layer would be due to older interstadials of MIS5, based on similar reasoning, all the dates should be indistinguishable from the background, since the peat layer should probably prevent intrusion of Holocenic carbon (and MIS3 layer would then not exist, since there are only two organic layers). Since we inarguably see effects of younger reworked carbon of MIS3 chronological horizon only and as a basal date inversion, we suggest that the layer is, indeed, due to MIS3. We note that the interpretation is tentative, as Holocenic influence that would suitably mix the gyttja to appear having MIS3 origin cannot be totally ruled out.

Since the twig samples are collected throughout the organic layer, one would expect a trend of decreasing age from the top to bottom if the layer was corresponding to the whole MIS3 period of ca. 24–59 cal kBP (Martinson et al., 1987). However, all the macrofossil twig (T1-T5) samples provide ^{14}C levels indistinguishable from the process background without such a trend. Slight deviation from this may be seen for T3 as $F_{uncorr,T3} = 0.0040(2)$ that differs statistically ($z = 10.6$, $p = 0$) from the average of the other twig samples T1,2,4,5 i.e. $F_{uncorr,\ ave\ T1,2,4,5} = 0.0014(2)$. We consider the T3 sample providing a lower limit for the overall age of the organic layer, this representing a depth of 13–15 cm from the top of the organic layer to date to ca. 45500 BP (F+2σ). Based on this interpretation, large lower-lying part of the sampled organic layer would date to the early MIS3 phases.

Quantitative temperature reconstructions from nearby Sokli (67°48′ N, 29°18’ E) indicate similar temperatures of early MIS3 than prevailing presently (Helmens et al., 2009). Our new data is chronologically coherent with this interpretation with the indication that the deposit was formed during a long period of tens of thousands of years, the most of the studied material corresponding to period older than 47600–53500 cal BP. Relying in the upper limit of the underlying clastic sediments provided by the OSL date, this concentration of dates would correspond to the early setting of MIS3 probably associated with the Greenland Interstadials (GI) of 14–17, identified within the ice core $\delta^{18}O$ records (Svensson et al., 2008). Particularly, the overall chronological estimate for MIS3 period of ca. 24000–59000 cal BP (Martinson et al., 1987) would constrain our chronological horizon for most of the dates to ca. 47600–59000 cal BP, coinciding the GI-14 (Fig. 1) dated to 48500–54500 cal BP (Van Meerbeeck et al., 2011). The two younger dates obtained here and by Sarala et al. (2016) (Fig. 6) could possibly correspond to GI-8, which is one of the most prominent interstadials during the later MIS3 period (Svensson et al., 2008).

4.5. Environmental setting

According to ice core $\delta^{18}O$ records from Greenland (Rasmussen et al., 2023), the $\delta^{18}O$ values were significantly lower for MIS3 than for MIS5 or Holocene indicating lower MIS3 temperatures at least in Greenland. In trees, potential temperature effect is essentially mediated by the soil water intake into tree and its leaves. It follows that comparisons between tree-ring and ice-core $\delta^{18}O$ records may be distorted by complexity of isotopic signal that is modified from the meteoric source water to formation of cellulose by isotopic enrichment in leaves due to transpiration of water, this ecophysiological process being related to photosynthetic stomatal control, and by isotopic exchange between leaf and xylem water (McCarroll and Loader, 2004; Roden et al., 2000). Indeed, mixed results have been obtained when comparing nearly modern wood cellulose $\delta^{18}O$ signal of *Larix* (Sidorova et al., 2010) to Greenland GISP2 ice core records (Meese et al., 1994). Whereas the tree-ring cellulose $\delta^{18}O$ signal from Yakutia (70° 62′ N, 147° 88′ E) correlated strongly with the Greenland ice core data, the Taimyr (71° 98′ N, 102° 47’ E) data revealed contrasting behavior (Sidorova et al., 2010). This implies non-uniform climatic patterns over the Arctic, these patterns being possibly also intermingled with local hydrological features linked to the onset/cessation of yearly growth of trees. Therefore, straightforward comparisons of oxygen isotopic records of these archives are challenging.

Within our $\delta^{18}O$ data, however, it is interesting that there are no differences between the observed values of the wood cellulose material in the Kaarreoja organic layer, of the *Pinus sylvestris* cellulose of the last 400 years within northern and eastern Finland (Hilasvuori et al., 2009), and of the cellulose of the old ^{14}C-free *Larix* (30/KAM/79) sample. This indicates similar environmental growth conditions having prevailed during the formation of the Kaarreoja organic deposit and those of recent (*Pinus*) and ancient (*Larix*) cellulose as observed in the eastern Fennoscandia. This is consistent with the suggestion of vegetation and temperature conditions that may have been very similar in all the MIS3 or MIS5c,e and Holocene stages, as observed at Sokli, northern Finland (Helmens, 2014; Helmens et al., 2009; Väliranta et al., 2009). As a caveat, the suggested similarity of temperature conditions over such a wide range of interglacial and interstadial stages largely diminishes the value of temperature correlations. That is, alternatively, given that

temperatures during the Odderade Interstadial (MIS5a) were not similar to other foregoing ice-free periods, our results would indicate that the conditions during which our sample materials were formed were not similar to those prevailing during the (MIS5a).

Furthermore, all the values from the eastern Fennoscandia – regardless of age and species - are ca. 5 ‰ and ca. 7 ‰ higher compared to the Taimyr ($\delta^{18}O_{TAY,\ mean} = 21.3$ ‰) and Yakutia ($\delta^{18}O_{YAK,\ mean} = 19.1$ ‰) signals recorded for the 20th century AD, respectively. The clearly higher $\delta^{18}O$ levels indicate that the temperature conditions during the formation of the Kaarreoja organic bed in northern Finland were more ameliorated than those within the northern Siberia of the last century. This $\delta^{18}O$ offset reflects probably the climatological differences between the European Arctic, affected by North Atlantic oceanic circulation patterns, and more continental northern Siberia.

5. Conclusions

Radiocarbon datings of the mid-Weichselian era samples, particularly of MIS3 chronological horizon, are challenging due to ^{14}C contents being close to the instrumental sensitivity limit. In this work, we provide large number of radiocarbon dates of an organic layer from river Lemmenjoki region, northern Finland, suspected to belong to MIS3, based on macrofossil-sized tree samples, bulk gyttja/peat samples with varying pretreatment processes, terrestrial twig/shrub samples and taking into account sample-size effects. Overall, the material and dates seem to correspond to the previously identified stratigraphical units of Sarala et al. (2016) characterized as peat/gyttja including wood pieces. Sample-size effects explain a part of the observed inconsistencies between the dates. However, the most significant influence is due to reworked carbon from younger material, particularly seen in basal layer dates. Therefore, special attention should be paid to use strong enough alkaline solutions in chemical pretreatment of samples, particularly of gyttja/peat, to minimize the effect. The large data set allows us to establish a chronological setting for the studied organic layer to be mostly due to early phases of the MIS3 period, possibly of GI-14 interstadial. Individual tree-sample finds provide also younger ages consistent to associating them tentatively with the GI-8 interstadial. Moreover, our data provides the glance into the tree-ring oxygen isotope records of the Weichselian glacial era. Isotope data indicate the growth conditions of the sampled trees having been nearly the similar compared to the last 400 years of the modern era within the Eastern Fennoscandia, emphasizing the persistent role of North Atlantic oceanic circulation patterns in defining the climate within the study area.

CRediT authorship contribution statement

Markku Oinonen: Writing – review & editing, Writing – original draft, Visualization, Validation, Supervision, Resources, Project administration, Methodology, Investigation, Funding acquisition, Formal analysis, Data curation, Conceptualization. **Laura Arppe:** Writing – review & editing, Validation, Methodology, Formal analysis, Data curation. **Joonas Uusitalo:** Writing – review & editing, Validation, Methodology, Investigation, Formal analysis, Data curation. **Samuli Helama:** Writing – review & editing, Writing – original draft, Resources, Methodology, Investigation, Conceptualization. **Pekka Nöjd:** Writing – review & editing, Supervision, Resources, Funding acquisition. **Harri Mäkinen:** Writing – review & editing, Investigation. **Pekka Saranpää:** Writing – review & editing, Validation, Methodology, Investigation, Formal analysis. **Kenichiro Mizohata:** Writing – review & editing, Validation, Methodology, Investigation, Formal analysis, Data curation.

Declaration of competing interest

The authors declare that they have no known competing financial interests or personal relationships that could have appeared to influence the work reported in this paper.

Acknowledgements

The authors would like to thank Ami Telilä for allowing for sampling the layer at his gold-mining site in Kaarreoja, Anne-Maija Forss for chemical pretreatments for ^{14}C analyses, Hanna Turunen and Igor Shevchuk for IRMS analyses, Kari Eskola for AMS sample combustions and graphitizations, and Pietari Kienanen for AMS analyses. The work was supported by the Research Council of Finland (Grant Nos. 288083 and 288267).

Data availability

Chronological data is available within the paper in Tables 1–4 The data on statistical comparisons will be made available on request.

References

Alexanderson, H., Eskola, K.O., Helmens, K.F., 2009. Optical dating of a late quaternary sediment sequence from Sokli, northern Finland. Geochronometria 32, 51–59. https://doi.org/10.2478/V10003-008-0022-9.

Andersen, K.K., Azuma, N., Barnola, J.M., Bigler, M., Biscaye, P., Caillon, N., Chappellaz, J., Clausen, H.B., Dahl-Jensen, D., Fischer, H., Flückiger, J., Fritzsche, D., Fujii, Y., Goto-Azuma, K., Grønvold, K., Gundestrup, N.S., Hansson, M., Huber, C., Hvidberg, C.S., Johnsen, S.J., Jonsell, U., Jouzel, J., Kipfstuhl, S., Landais, A., Leuenberger, M., Lorrain, R., Masson-Delmotte, V., Miller, H., Motoyama, H., Narita, H., Popp, T., Rasmussen, S.O., Raynaud, D., Rothlisberger, R., Ruth, U., Samyn, D., Schwander, J., Shoji, H., Siggard-Andersen, M.L., Steffensen, J. P., Stocker, T., Sveinbjörnsdóttir, A.E., Svensson, A., Takata, M., Tison, J.L., Thorsteinsson, T., Watanabe, O., Wilhelms, F., White, J.W.C., 2004. High-resolution record of Northern Hemisphere climate extending into the last interglacial period. Nature 431, 147–151. https://doi.org/10.1038/nature02805.

Bernabei, M., Bontadi, J., 2011. Distinguishing root- and stem-wood of Picea Abies. IAWA J. 32, 375–382. https://doi.org/10.1163/22941932-90000065.

Boettger, T., Haupt, M., Knöller, K., Weise, S.M., Waterhouse, J.S., Rinne, K.T., Loader, N.J., Sonninen, E., Jungner, H., Masson-Delmotte, V., Stievenard, M., Guillemin, M.T., Pierre, M., Pazdur, A., Leuenberger, M., Filot, M., Saurer, M., Reynolds, C.E., Helle, G., Schleser, G.H., 2007. Wood cellulose preparation methods and mass spectrometric analyses of δ13C, δ18O, and nonexchangeable δ2H values in cellulose, sugar, and starch: an interlaboratory comparison. Anal. Chem. 79, 4603–4612. https://doi.org/10.1021/AC0700023/SUPPL_FILE/AC0700023SI20070326_112410.XLS.

Bonhommet, N., Zähringer, J., 1969. Paleomagnetism and potassium argon age determinations of the Laschamp geomagnetic polarity event. Earth Planet Sci. Lett. 6, 43–46. https://doi.org/10.1016/0012-821X(69)90159-9.

de Vries, H.L., Barendsen, G.W., 1954. Measurements of Age by the Carbon-14 technique. Nature 174, 1138–1141. https://doi.org/10.1038/1741138a0.

Donahue, D.J., Jull, A.J.T., Toolin, L.J., 1990. Radiocarbon measurements at the University of Arizona AMS facility. Nucl. Instrum. Methods Phys. Res. B 52, 224–228. https://doi.org/10.1016/0168-583X(90)90410-V.

Hättestrand, M., Robertsson, A.M., 2010. Weichselian interstadials at Riipiharju, northern Sweden – interpretation of vegetation and climate from fossil and modern pollen records. Boreas 39, 296–311. https://doi.org/10.1111/J.1502-3885.2009.00129.X.

Helama, S., Arppe, L., Timonen, M., Mielikäinen, K., Oinonen, M., 2015. Age-related trends in subfossil tree-ring δ13C data. Chem. Geol. 416, 28–35. https://doi.org/10.1016/j.chemgeo.2015.10.019.

Hellberg, E., Carcaillet, C., 2016. Wood anatomy of West European Betula: quantitative descriptions and applications for routine identification in paleoecological studies. https://doi.org/10.1080/11956860.2003.1168278610, 370-379. https://doi.org/10.1080/11956860.2003.11682786.

Helmens, K.F., 2014. The last interglacial-glacial cycle (MIS 5-2) re-examined based on long proxy records from central and northern Europe. Quat. Sci. Rev. 86, 115–143. https://doi.org/10.1016/j.quascirev.2013.12.012.

Helmens, K.F., Risberg, J., Jansson, K.N., Weckström, J., Berntsson, A., Tillman, P.K., Johansson, P.W., Wastegård, S., 2009. Early MIS 3 glacial lake evolution, ice-marginal retreat pattern and climate at Sokli (northeastern Fennoscandia). Quat. Sci. Rev. 28, 1880–1894. https://doi.org/10.1016/J.QUASCIREV.2009.03.001.

Hilasvuori, E., Berninger, F., Sonninen, E., Tuomenvirta, H., Jungner, H., 2009. Stability of climate signal in carbon and oxygen isotope records and ring width from Scots pine (*Pinus sylvestris* L.) in Finland. J. Quat. Sci. 24, 469–480. https://doi.org/10.1002/jqs.1260.

Kalm, V., 2006. Pleistocene chronostratigraphy in Estonia, southeastern sector of the Scandinavian glaciation. Quat. Sci. Rev. 25, 960–975. https://doi.org/10.1016/j.quascirev.2005.08.005.

Kasso, T.M., Oinonen, M.J., Mizohata, K., Tahkokallio, J.K., Heikkilä, T.M., 2021. Volumes of Worth—Delimiting the sample size for radiocarbon dating of parchment. Radiocarbon 63, 105–120. https://doi.org/10.1017/RDC.2020.128.

Kozakiewicz, P., Zyczkowski, W., 2015. Physical and mechanical properties and anatomy of common juniper (Juniperus communis L.) wood. Sylwan 159, 151–159.

Lunkka, J.P., Murray, A., Korpela, K., 2008. Weichselian sediment succession at Ruunaa, Finland, indicating a Mid-Weichselian ice-free interval in eastern Fennoscandia. Boreas 37, 234–244. https://doi.org/10.1111/J.1502-3885.2007.00021.X.

Lunkka, J.P., Sarala, P., Gibbard, P.L., 2015. The Rautuvaara section, western Finnish Lapland, revisited – new age constraints indicate a complex Scandinavian Ice Sheet history in northern Fennoscandia during the Weichselian Stage. Boreas 44, 68–80. https://doi.org/10.1111/BOR.12088.

Mäkinen, K., 2005. Dating the Weichselian deposits of southwestern Finnish Lapland. Geol. Surv. Finland, Spec. Pap. 40, 67–78 https://doi.org/10.0/FONT/BOOTSTRAP-ICONS.MIN.CSS.

Mäkinen, K., 1982. Tiedonanto Vuotson interglasiaalisesta lehtikuusen rungosta [Report on interglacial Larix trunk at Vuotso, Northern Finland]. Geologi 34, 182–184.

Martinson, D.G., Pisias, N.G., Hays, J.D., Imbrie, J., Moore, T.C., Shackleton, N.J., 1987. Age dating and the orbital theory of the ice ages: development of a high-resolution 0 to 300,000-year chronostratigraphy. Quat. Res. 27, 1–29. https://doi.org/10.1016/0033-5894(87)90046-9.

McCarroll, D., Loader, N.J., 2004. Stable isotopes in tree rings. Quat. Sci. Rev. 23, 771–801. https://doi.org/10.1016/J.QUASCIREV.2003.06.017.

Meese, D.A., Gow, A.J., Grootes, P., Mayewski, P.A., Ram, M., Stuiver, M., Taylor, K.C., Waddington, E.D., Zielinski, G.A., 1994. The accumulation record from the GISP2 core as an indicator of climate change throughout the Holocene. Science (266), 1680–1682. https://doi.org/10.1126/SCIENCE.266.5191.1680, 1979.

Palonen, V., 2008a. Accelerator Mass Spectrometry and Bayesian Data Analysis. University of Helsinki.

Palonen, V., 2008b. Accelerator Mass Spectrometry and Bayesian Data Analysis. University of Helsinki.

Palonen, V., Pesonen, A., Herranen, T., Tikkanen, P., Oinonen, M., 2013. HASE - the Helsinki adaptive sample preparation line. In: Nuclear Instruments and Methods in Physics Research, Section B: Beam Interactions with Materials and Atoms, pp. 182–184. https://doi.org/10.1016/j.nimb.2012.08.056.

Palonen, V., Tikkanen, P., 2015. A novel upgrade to Helsinki AMS: fast switching of isotopes with electrostatic deflectors. Nucl. Instrum. Methods Phys. Res. B 361, 263–266. https://doi.org/10.1016/j.nimb.2015.04.053.

Palonen, V., Tikkanen, P., Keinonen, J., 2010a. Using car4ams, the bayesian ams data analysis code. Radiocarbon 52, 948–952. https://doi.org/10.1017/S0033822200046051.

Palonen, V., Tikkanen, P., Keinonen, J., 2010b. Improving AMS uncertainties and detection of instrumental error. Nucl. Instrum. Methods Phys. Res. B 268, 972–975. https://doi.org/10.1016/j.nimb.2009.10.077.

Palstra, S.W.L., Wallinga, J., Viveen, W., Schoorl, J.M., van den Berg, M., van der Plicht, J., 2021. Cross-comparison of last glacial radiocarbon and OSL ages using periglacial fan deposits. Quat. Geochronol. 61, 101128. https://doi.org/10.1016/J.QUAGEO.2020.101128.

Rasmussen, S.O., Bigler, M., Blockley, S.P., Blunier, T., Buchardt, S.L., Clausen, H.B., Cvijanovic, I., Dahl-Jensen, D., Johnsen, S.J., Fischer, H., Gkinis, V., Guillevic, M., Hoek, W.Z., Lowe, J.J., Pedro, J.B., Popp, T., Seierstad, I.K., Steffensen, J.P., Svensson, A.M., Vallelonga, P., Vinther, B.M., Walker, M.J.C., Wheatley, J.J., Winstrup, M., 2014. A stratigraphic framework for abrupt climatic changes during the last Glacial period based on three synchronized Greenland ice-core records: refining and extending the INTIMATE event stratigraphy. Quat. Sci. Rev. 106, 14–28. https://doi.org/10.1016/J.QUASCIREV.2014.09.007.

Rasmussen, S.O., Dahl-Jensen, D., Fischer, H., Fuhrer, K., Hansen, S.B., Hansson, M., Hvidberg, C.S., Jonsell, U., Kipfstuhl, S., Ruth, U., Schwander, J., Siggaard-Andersen, M.L., Sinnl, G., Steffensen, J.P., Svensson, A.M., Vinther, B.M., 2023. Ice-core data used for the construction of the Greenland Ice-Core Chronology 2005 and 2021 (GICC05 and GICC21). Earth Syst. Sci. Data 15, 3351–3364. https://doi.org/10.5194/ESSD-15-3351-2023.

Reimer, P.J., Austin, W.E.N., Bard, E., Bayliss, A., Blackwell, P.G., Bronk Ramsey, C., Butzin, M., Cheng, H., Edwards, R.L., Friedrich, M., Grootes, P.M., Guilderson, T.P., Hajdas, I., Heaton, T.J., Hogg, A.G., Hughen, K.A., Kromer, B., Manning, S.W., Muscheler, R., Palmer, J.G., Pearson, C., van der Plicht, J., Reimer, R.W., Richards, D.A., Scott, E.M., Southon, J.R., Turney, C.S.M., Wacker, L., Adolphi, F., Büntgen, U., Capano, M., Fahrni, S.M., Fogtmann-Schulz, A., Friedrich, R., Köhler, P., Kudsk, S., Miyake, F., Olsen, J., Reinig, F., Sakamoto, M., Sookdeo, A., Talamo, S., 2020. The IntCal20 Northern Hemisphere radiocarbon age calibration curve (0–55 Cal kBP). Radiocarbon 1–33. https://doi.org/10.1017/RDC.2020.41.

Roden, J.S., Lin, G., Ehleringer, J.R., 2000. A mechanistic model for interpretation of hydrogen and oxygen isotope ratios in tree-ring cellulose. Geochem. Cosmochim. Acta 64, 21–35. https://doi.org/10.1016/S0016-7037(99)00195-7.

Salonen, V.P., Kaakinen, A., Kultti, S., Miettinen, A., Eskola, K.O., Lunkka, J.P., 2008. Middle Weichselian glacial event in the central part of the Scandinavian Ice Sheet recorded in the Hitura pit, Ostrobothnia, Finland. Boreas 37, 38–54. https://doi.org/10.1111/J.1502-3885.2007.00009.X.

Salonen, V.P., Moreau, J., Hyttinen, O., Eskola, K.O., 2014. Mid-Weichselian interstadial in Kolari, western Finnish Lapland. Boreas 43, 627–638. https://doi.org/10.1111/BOR.12060.

Sarala, P., Eskola, T., 2011. Middle Weichselian interstadial deposit at Petäjäselkä, Northern Finland. Quat. Sci. J. 60, 488–492. https://doi.org/10.3285/EG.60.4.07.

Sarala, P., Pihlaja, J., Putkinen, N., Murray, A., 2010. Composition and origin of the Middle Weichselian interstadial deposit in Veskoniemi, northern Finland. Est. J. Earth Sci. 59, 117–124. https://doi.org/10.3176/EARTH.2010.2.02.

Sarala, P., Väliranta, M., Eskola, T., Vaikutiené, G., 2016. First physical evidence for forested environment in the Arctic during MIS 3. Sci. Rep. 6, 1–9. https://doi.org/10.1038/srep29054.

Schweingruber, F.H., 1990. Microscopic Wood Anatomy Mikroskopische Holzanatomie, Anatomie Microscopique Du Bois, 3rd ed. Wald, Schnee und Landshaft.

Scott, E.M., Naysmith, P., Cook, G.T., 2017. Should archaeologists care about 14C Intercomparisons? Why? A Summary report on SIRI. Radiocarbon 59, 1589–1596. https://doi.org/10.1017/RDC.2017.12.

Sidorova, O.V., Siegwolf, R.T.W., Saurer, M., Naurzbaev, M.M., Shashkin, A.V., Vaganov, E.A., 2010. Spatial patterns of climatic changes in the Eurasian north reflected in Siberian larch tree-ring parameters and stable isotopes. Glob. Change Biol. 16, 1003–1018. https://doi.org/10.1111/J.1365-2486.2009.02008.X.

Slota, P.J., Jull, A.J.T., Linick, T.W., Toolin, L.J., 1987. Preparation of small samples for 14 C accelerator targets by catalytic reduction of CO. Radiocarbon. https://doi.org/10.1017/s0033822200056988.

Stirling, C.H., Esat, T.M., Lambeck, K., McCulloch, M.T., 1998. Timing and duration of the Last Interglacial: evidence for a restricted interval of widespread coral reef growth. Earth Planet Sci. Lett. 160, 745–762. https://doi.org/10.1016/S0012-821X(98)00125-3.

Svensson, A., Andersen, K.K., Bigler, M., Clausen, H.B., Dahl-Jensen, D., Davies, S.M., Johnsen, S.J., Muscheler, R., Parrenin, F., Rasmussen, S.O., Röthlisberger, R., Seierstad, I., Steffensen, J.P., Vinther, B.M., 2008. A 60 000 year Greenland stratigraphic ice core chronology. Clim. Past 4, 47–57. https://doi.org/10.5194/cp-4-47-2008.

Tikkanen, P., Palonen, V., Jungner, H., Keinonen, J., 2004. AMS facility at the University of Helsinki. Nucl. Instrum. Methods Phys. Res. B 223–224, 35–39. https://doi.org/10.1016/j.nimb.2004.04.011.

Uusitalo, J., Arppe, L., Hackman, T., Helama, S., Kovaltsov, G., Mielikäinen, K., Mäkinen, H., Nöjd, P., Palonen, V., Usoskin, I., Oinonen, M., 2018. Solar superstorm of AD 774 recorded subannually by Arctic tree rings. Nat. Commun. 9, 3495. https://doi.org/10.1038/s41467-018-05883-1.

Uusitalo, J., Arppe, L., Helama, S., Mizohata, K., Mielikäinen, K., Mäkinen, H., Nöjd, P., Timonen, M., Oinonen, M., 2022. From lakes to ratios: 14C measurement process of the Finnish tree-ring research consortium. Nucl. Instrum. Methods Phys. Res. B 519, 37–45. https://doi.org/10.1016/J.NIMB.2022.03.013.

Väliranta, M., Birks, H.H., Helmens, K., Engels, S., Piirainen, M., 2009. Early Weichselian interstadial (MIS 5c) summer temperatures were higher than today in northern Fennoscandia. Quat. Sci. Rev. 28, 777–782. https://doi.org/10.1016/j.quascirev.2009.01.004.

van der Plicht, J., Hogg, A., 2006. A note on reporting radiocarbon. Quat. Geochronol. 1, 237–240. https://doi.org/10.1016/j.quageo.2006.07.001.

Van Meerbeeck, C.J., Renssen, H., Roche, D.M., Wohlfarth, B., Bohncke, S.J.P., Bos, J.A.A., Engels, S., Helmens, K.F., Sánchez-Goñi, M.F., Svensson, A., Vandenberghe, J., 2011. The nature of MIS 3 stadial-interstadial transitions in Europe: new insights from model-data comparisons. Quat. Sci. Rev. 30, 3618–3637. https://doi.org/10.1016/j.quascirev.2011.08.002.

Wohlfarth, B., 2010. Ice-free conditions in Sweden during marine oxygen isotope stage 3? Boreas 39, 377–398. https://doi.org/10.1111/j.1502-3885.2009.00137.x.